



ELSEVIER

15 January 1998

OPTICS  
COMMUNICATIONS

Optics Communications 146 (1998) 201–207

# Dynamics of an optical resonator determined by its iterative map of beam parameters

Ming-Dar Wei<sup>a</sup>, Wen-Feng Hsieh<sup>a,\*</sup>, C.C. Sung<sup>b</sup><sup>a</sup> Institute of Electro-Optical Engineering, National Chiao Tung University, Ta-Hsueh Rd. 1001, Hsinchu 30050, Taiwan<sup>b</sup> Physics Department, University of Alabama, Huntsville, AL 35899, USA

Received 29 April 1997; revised 8 September 1997; accepted 8 September 1997

---

## Abstract

We use the residue of the map to study the stability and Gaussian beam dynamics of a general optical resonator. The map is constructed from space domain matrix formalism. For a lossless system we find that the residue is a function of resonator  $g$ -parameters' product and new critical stable curves exist within the geometrically stable regions. The dynamic behavior of a dissipative resonator with loss optical element is similar to a damping oscillatory motion and can be determined by the corresponding conservative resonator without those loss elements. © 1998 Elsevier Science B.V.

PACS: 42.60.D

Keywords: Resonators; Dynamics; Stability; Gaussian beam

---

## 1. Introduction

The ABCD matrix formalism is a very useful tool to deal with the propagation of a Gaussian beam in periodical media to characterize laser resonators. The mode confinement referring to the existence of a spatially confined beam within the resonator has been used as a criterion for cavity design [1]. Owing to the inherent clock provided by the round-trip time of the optical resonator, recently an approach borrowed from the nonlinear dynamics is adopted to derive the iterative map from beam parameters to study the dynamics of laser resonators [2,3]. The dynamics of the beam parameters (spot size, radius of curvature and beam quality factor  $M^2$ ) have intrinsically complex behaviors obtained by the bare resonators without invoking the effect of the laser medium [2]. Although the reasons for the complex behaviors are not clear, these behaviors have been classified into three classes in Ref. [2]: (i) monotonic evolution; (ii) damped oscillations on a few frequencies;

and (iii) quite complicated evolution. They found that these maps were endowed with the fixed stable point, physically representing the values of beam parameters at steady state. On the other hand, a five-dimension iterative map was used to discuss the dynamically stable regions of self mode locking lasers. These five dimensions correspond to spot size, radius of curvature, chirp, pulse duration and energy. The results agree with experimental data [3]. Therefore, analyzing the map of Gaussian beam parameters offers an approach to study the dynamic evolutions of the beam parameters and the stability of the resonators.

In order to understand the complex dynamic evolution and stability of a resonator, we construct a simple two-dimensional iterative map related to the spot size and radius of curvature. The complex dynamic behavior of the map can be determined by the residue which is defined as a function of the trace of its Jacobian matrix [4]. As a result, the residue is a function of the product of  $g$ -parameters of a general resonator. We found new critical stable curves within the geometrically stable regions. These critical stable curves correspond to the product of wide-spread res-

---

\* Corresponding author. E-mail: wfhsieh@cc.nctu.edu.tw.

onator  $g$ -parameters equal to  $1/2$  which cannot be found by ray tracing directly. When we add a loss-like effect, such as adding a Gaussian aperture, the numerical calculated evolution of the spot size is a damping oscillatory motion with the same period of oscillation as the lossless resonator. In addition, we can explain the behavior of the complex dynamics [2] of bare resonators by the residues of the corresponding conservative maps. The numerical results demonstrate that “the damped oscillation” and “quite complicated” evolution in Ref. [2] are just associated with the short and long period oscillatory motions, and the “quite complicated” evolution is an overdamping result under loss-like effect.

## 2. Theory

When the Gaussian beam propagates through an optical element, its  $q$ -parameter will transform according to the ABCD law [1]. The  $q$ -parameter is given by  $1/q = 1/R - i\lambda/\pi w^2$ , where  $R$  is the radius of curvature,  $w$  is the spot size, and  $\lambda$  is the wavelength of resonator beam. Assuming that

$$\begin{bmatrix} A & B \\ C & D \end{bmatrix}$$

is the round-trip transfer matrix and the reference plane is chosen to be just before the beam hitting one of the two end mirrors, by applying the ABCD law, we can relate the  $q$ -parameter of the  $(n+1)$ th round-trip to the  $n$ th one as

$$R_{n+1} = \left( \operatorname{Re} \left[ \frac{C + D(1/R_n - i\lambda/\pi w_n^2)}{A + B(1/R_n - i\lambda/\pi w_n^2)} \right] \right)^{-1}, \quad (1)$$

and

$$w_{n+1} = \left( -\frac{\pi}{\lambda} \operatorname{Im} \left[ \frac{C + D(1/R_n - i\lambda/\pi w_n^2)}{A + B(1/R_n - i\lambda/\pi w_n^2)} \right] \right)^{-2} \quad (2)$$

where the  $\operatorname{Re}$  and  $\operatorname{Im}$  represent the real and imaginary parts of a complex number.

For a lossless resonator, the system identified with the classical ray equation is conservative with real transfer matrix [5]. The laws of transformation of Gaussian beams are formally identical to those of ray pencils [6]. The map derived from the beam parameters (curvature and spot size only) of the lossless resonator belongs to the conservative one and can be written as

$$\begin{aligned} R_{n+1} &= f(R_n, w_n) \\ &= \frac{(A + B/R_n)^2 + (\lambda/\pi w_n^2)^2 B^2}{(A + B/R_n)(C + D/R_n) + (\lambda/\pi w_n^2)^2 BD}, \end{aligned} \quad (3)$$

and

$$\begin{aligned} w_{n+1} &= h(R_n, w_n) \\ &= w_n \sqrt{(A + B/R_n)^2 + (\lambda/\pi w_n^2)^2 B^2}. \end{aligned} \quad (4)$$

It represents a two-dimensional iterative map, and the discrete time interval of the map is equal to one round-trip time of the resonator. This is the same procedure to analyze a nonlinear dynamic system from continuous time to discrete one. The fixed point is the self-consistent solution of  $q$ -parameter, i.e., the steady-state solution [1]. Under linear stability analysis, the stability of the fixed point is determined by its Jacobian eigenvalues of the map [7]. Discussing the Jacobian eigenvalues of the map at the fixed point is equivalent to determine the dynamic stability of laser resonators.

Because the map belongs to a conservative one, the determinant of the Jacobian matrix equals unity and the eigenvalues of the Jacobian matrix depend only on the trace. It is convenient to discuss the stability using the residue, which is defined as [4]

$$\operatorname{Res} = \frac{1}{4} [2 - \operatorname{Tr}(M_J)], \quad (5)$$

where  $M_J$  is the Jacobian matrix and  $\operatorname{Tr}(M_J)$  is its trace. When  $0 < \operatorname{Res} < 1$ , the eigenvalues are complex with unity magnitude and tangent space orbits rotate about the fixed point on ellipses and the system is stable. The relation between residue and the phase shift per iteration of the map,  $\theta$ , can be represented as

$$\operatorname{Res} = \sin^2(\theta/2). \quad (6)$$

Whereas the system is unstable with either  $\operatorname{Res} < 0$  or  $\operatorname{Res} > 1$ , its tangent space orbit locates on a hyperbola.

In standing wave resonators with real round-trip transfer matrices the curvatures of the resonator beam must match those of the end mirrors. From Eqs. (3) to (5), the residue is

$$\operatorname{Res} = 1 - (A + B/\rho_1)^2 = 1 - (2G_1 G_2 - 1)^2. \quad (7)$$

Here we have defined  $G_1 = a - b/\rho_1$  and  $G_2 = d - b/\rho_2$  as the  $G$ -parameters for general optical resonators, with

$$\begin{bmatrix} a & b \\ c & d \end{bmatrix}$$

the transfer matrix of one-way pass between the two end mirrors, and  $\rho_1, \rho_2$  is the radii of curvature about the two end mirrors, respectively. So we can obtain a convenient method to discuss the stability of multiple-element resonators using the  $G$ -parameters defined above.

For simplicity, we apply this result to discuss the stability of a simple two-mirror resonator. This simplest kind of optical resonator consists of only two end mirrors

facing each other. The transfer matrix of one-way pass between two end mirrors is

$$\begin{bmatrix} 1 & L \\ 0 & 1 \end{bmatrix},$$

where  $L$  is the separation of the two end mirrors. We obtain

$$\text{Res} = 1 - (2g_1g_2 - 1)^2, \tag{8}$$

where  $g_i = 1 - L/\rho_i$  with  $i = 1, 2$  and again  $\rho_1$  and  $\rho_2$  are the radii of the two end-mirrors, respectively. From Eq. (8), we found that the residue is a function of  $g_1g_2$  only. Thus we plot the residue versus  $g_1g_2$  with solid line in Fig. 1, it is a parabola and its top locates on  $g_1g_2 = 1/2$  with  $\text{Res} = 1$ . The tendency of  $\theta$  is also shown in Fig. 1 with dashed line, which is also symmetrical to the maximum value at  $g_1g_2 = 1/2$ . We will depict in Section 3 that the dynamic behavior is mainly determined by the residue and  $\theta$  from comparing the numerical results with theoretical analysis.

Since the resonator is dynamically unstable for  $\text{Res} < 0$  or  $\text{Res} > 1$ , one gets regions with  $g_1g_2 < 0$  or  $g_1g_2 > 1$ . And the region with  $0 < g_1g_2 < 1$  is stable corresponding to  $0 < \text{Res} < 1$ . It is critical stable with  $\text{Res} = 0$  for  $g_1g_2 = 0$  or  $g_1g_2 = 1$ . The stability of these regions are the same as the geometrical stability ones. The geometrical stability regions can be found in a general textbook [1], the resonator is stable in the region  $0 < g_1g_2 < 1$  and critical stable on the borderlines  $g_1g_2 = 0$  and  $g_1g_2 = 1$ . However, extra critical curves are found within the geometrically stable regions  $0 < g_1g_2 < 1$  where  $0 < \text{Res} < 1$ . The curves are  $g_1g_2 = 1/2$  with  $\text{Res} = 1$ . This result can not be found by ray tracing method. Stability range decided by the iterative map of the beam parameters not only implies geometrical stability range but also has an extra dynamically critical stable solution with  $g_1g_2 = 1/2$ . For the sake of comparing the properties of these critical resonators, we show the configurations of resonators with ray tracing in Fig. 2. A symmetric confocal resonator with  $g_1 = g_2 = 0$  is shown in Fig. 2(a), the center of curvature

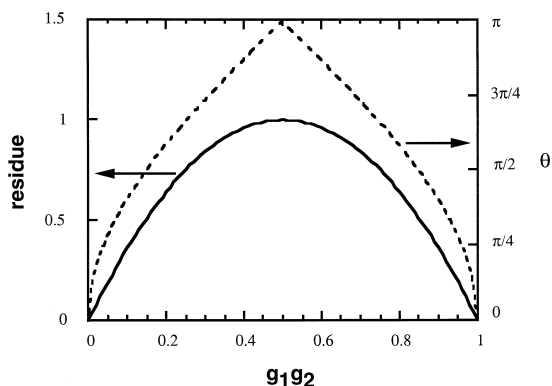


Fig. 1. The calculated residue and average angle of rotation versus the product of  $g$ -parameters. The maximum values appears at  $g_1g_2 = 1/2$ .

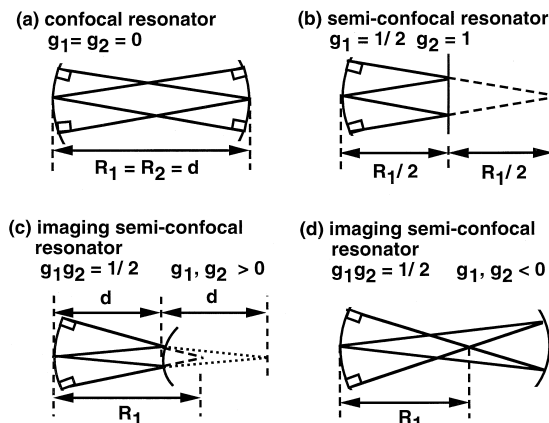


Fig. 2. Diagram of critical stable resonators, (a) confocal, (b) semi-confocal, and imaging semi-confocal resonators in both positive (c) and negative (d) branches, respectively.

of one mirror locates at the center of the other mirror. And the configuration with  $g_1 = 1/2$  and  $g_2 = 1$ , as shown in Fig. 2(b), is half of the symmetric confocal resonator and named ‘‘semi-confocal’’ [8]. We call the resonator configurations with  $g_1g_2 = 1/2$  as ‘‘imaging semi-confocal’’ resonators. Both positive and negative configurations branches are plotted in Figs. 2(c) and 2(d), respectively. In either one of these resonators, any arbitrary ray returns to its initial value after four round trips rather than just double round trips for confocal configuration at  $g_1 = g_2 = 0$ . And the semi-confocal resonator is just a special case of the imaging semi-confocal one with  $g_1g_2 = 1/2$ .

Since the fundamental transverse mode cannot efficiently enough extract the stored energy in the gain medium, in the confocal resonators can support more or less arbitrary multi-transverse modes [1]. As mentioned above, the geometrical configuration of the imaging semi-confocal resonators is half of the confocal one. We will expect that imaging semi-confocal resonators have properties similar to the confocal resonators. The multi-transverse mode pattern and output power drop may be observed in imaging semi-confocal resonators. In fact, we had observed power drop near  $G_1G_2 = 1/2$  in a Kerr-lens mode-locking (KLM) Ti:sapphire laser [9] and multi-transverse modes within this region by forward study. The same result is also obtained from the diode-pumped Nd:YVO<sub>4</sub> solid-state laser and will be presented elsewhere. And this region is about hundreds of micrometers different from the cavity length. In general, we adjust the resonator for purposing the maximum output power, it is easy to avoid this effect to keep away from operating at the power drop region. Besides, we could apply this condition to design a resonator to prefer one operation mode than the other through gain competition. For example, for the KLM laser if we design the resonator for cw mode acting at  $G_1G_2 = 1/2$ , the equivalent resonator of KLM mode will apart from having  $G_1G_2 = 1/2$  due to the change of effective

cavity length via optical Kerr effect. Thus, the KLM mode is capable to extract more stored energy from the gain medium in this resonator.

Real systems often have nonlinear effect such as saturated gain, mode coupling, or optical Kerr effect. If a nonlinear term is added to perturb this critical stable system having  $\text{Res} = 1$ , the Poincare-Birkhoff theorem tells us that some of period 2 fixed points in  $\text{Res} = 1$  (with  $\theta = \pi$ ) survive the perturbation, producing the bifurcation phenomena [7]. So this system will be sensitive to nonlinear effect and subject to fluctuation. The particular significance of “critical stable” exists accompanied with nonlinear effect. Whereas the steady-state solution corresponds to the ensemble average of the map evolution. The average steady-state value cannot imply dynamical fluctuation of the system. The spot size to the geometrical perturbation discussed in Ref. [1] is an approach considering the variation of the steady-state spot size. Although the variation of the steady-state spot size to the geometrical perturbation is equal to zero at  $g_1 g_2 = 1/2$ , the dynamical fluctuation is nonzero. We believe that the system is noisy but its average spot size is insensitive to the variation of geometrical configuration near  $g_1 g_2 = 1/2$  under the nonlinear effect. In addition, the resonator with nonlinear effect at this critical structure may be also responsible for the observed chaotic behavior [10].

### 3. Numerical results

In this section, we will numerically discuss the iterative maps of both dynamic systems having complex and real transfer matrices. In a complex matrix system, the evolution of a Gaussian beam corresponds to a dissipative system [4] and its phase exhibits a damped (or growing) oscillatory behavior [11]. It is different from the real transfer matrix system corresponding to the ray pencil conservative system. By considering a Gaussian aperture as a lossy optical element, the evolution of the spot size with and without this lossy element will be compared.

First, let us consider a lossless resonator formed by a flat and a spherical mirror. Again one chooses the reference plane as that just before the beam hits the flat mirror. Fig. 3(a) represents 5000 iterations of the map determined by Eqs. (3) and (4) for  $g_1 g_2 = 0.9$ , the initial value is arbitrary chosen as  $1/R_0 = 0$  and  $w_0 = 1.5$  mm. From Eqs. (6) and (8), we obtain that the residue of this resonator is 0.36 and  $\theta \approx 0.41\pi$ . Because the iterative map belongs to the conservative one and the phase shift per iteration is not a rational fraction of  $2\pi$ , the figure shows a close loop. Since the phase shift per iteration is approximately equal to  $0.41\pi$  which is about  $0.01\pi$  greater than the closest rational fraction phase shift  $2\pi/5$ , it represents that the iterative point will return to the neighborhood of the initial point after five iterations. So the evolution of the

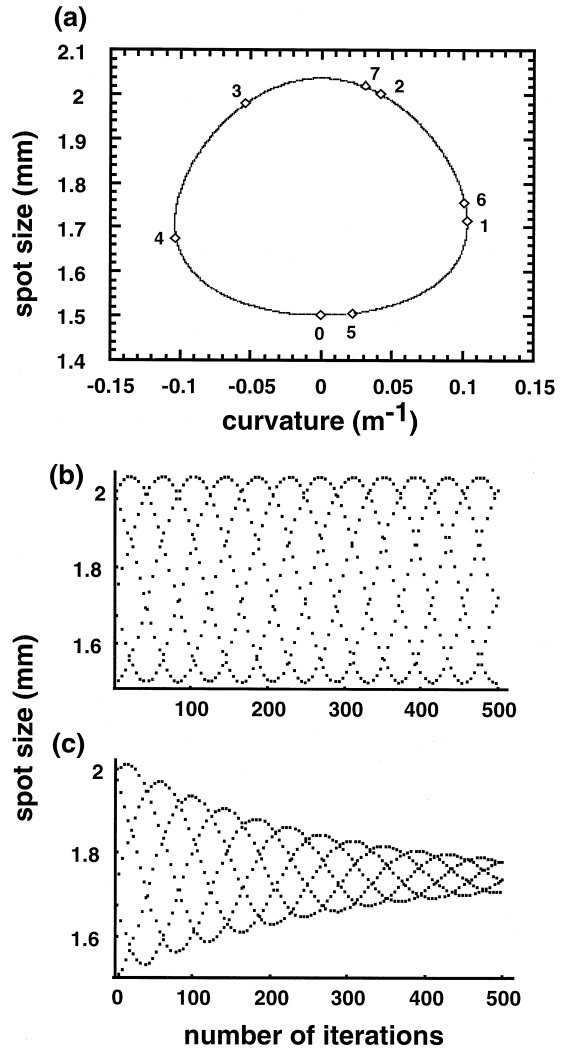


Fig. 3. Evolution of the iterative map for  $g_1 g_2 = 0.9$  with initial values  $(1/R_0, w_0) = (0, 1.5)$ . (a) Two-dimensional map for real round-trip transfer matrix, the diamonds mark the number corresponding to the first 7 iterations. (b) The evolution of spot size versus the number of iterations for the same map as (a). (c) The evolution of spot size versus the number of iterations for a Gaussian aperture with transverse coefficient  $a_2 = 10^4 \text{ m}^{-2}$ .

spot size will develop into five groups and the behavior of each group acts like an oscillatory motion. The relative phase shift is  $0.41\pi$  between the neighboring trajectories. From each oscillatory trajectory composed of every other five iterations, there is  $5 \times 0.01\pi$  preceding phase difference after five iterations which equals to  $0.01\pi$  average preceding phase difference per iteration. Whence the period of each trajectory equals to  $2\pi$  divided by the absolute value of average phase difference per iteration,  $|\theta - 2\pi/n|$  ( $0.01\pi$  in this case), the period of the oscillatory

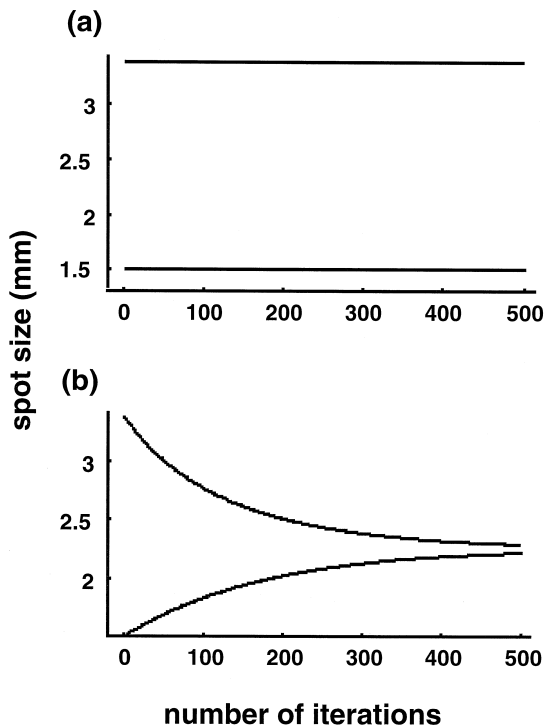


Fig. 4. Evolution of spot size for  $g_1 g_2 = 1/2$  with initial values  $(1/R_0, w_0) = (0, 1.5)$ . (a) Conservative system and (b) with a Gaussian aperture corresponding to  $a_2 = 10^4 \text{ m}^{-2}$ .

trajectory can be calculated from

$$\text{period} = \frac{2\pi}{|\theta - 2\pi/n|}, \tag{9}$$

where  $2\pi/n$  is the closest rational fraction rotation angle. The diamond marks in Fig. 3(a) show the first 7 iterations beginning from the initial state. The 5th iteration is neighbor of the initial point and also leads to the initial point as predicted by theoretical calculation. The same result is plotted in Fig. 3(b) as the evolution of spot size versus the number of iterations. We found five oscillatory trajectories having relative phase shift about  $1/5$  period (corresponding to  $0.41\pi$ ) between the neighboring ones. From Eq. (9) with  $n = 5$ , we get that the period of every oscillatory trajectory is about 207 iterations. It agrees well with the numerical result in Fig. 3(b).

When we add a Gaussian aperture in front of the flat mirror, the complex transfer matrix of the Gaussian aperture is

$$\begin{bmatrix} 1 & 0 \\ -i\lambda a_2/2\pi & 1 \end{bmatrix},$$

where  $a_2$  is the transverse coefficient [1]. Because the round trip transfer matrix is complex, one must use the iterative map of Eqs. (1) and (2) instead of Eqs. (3) and (4). Fig. 3(c) depicts the numerical evolution of spot size

versus the number of iterations. The initial value is  $(1/R_0, w_0) = (0, 1.5)$  and transverse coefficient  $a_2 = 10^4 \text{ m}^{-2}$  which is related to  $\sqrt{2}$  cm of  $1/e$  radius of the amplitude transmission through the aperture. We find that the evolution is an underdamping oscillatory motion with the same period of oscillation as in the lossless system. The properties of the lossy optical elements for the iterative map are similar to the effects of damping parameters in damping harmonic oscillators. The dynamic behavior of such a dissipative resonator is determined by the corresponding conservative resonator without those loss elements.

For the phase shift per iteration of the resonator having a rational fraction of  $2\pi$ , the iterative point will exactly return to its initial point after some iterations. For example, for the critical stable resonator with  $g_1 g_2 = 1/2$  (where  $\text{Res} = 1$  and  $\theta = \pi$ ), the iterative point will return to its initial point after two iterations and repeat itself every

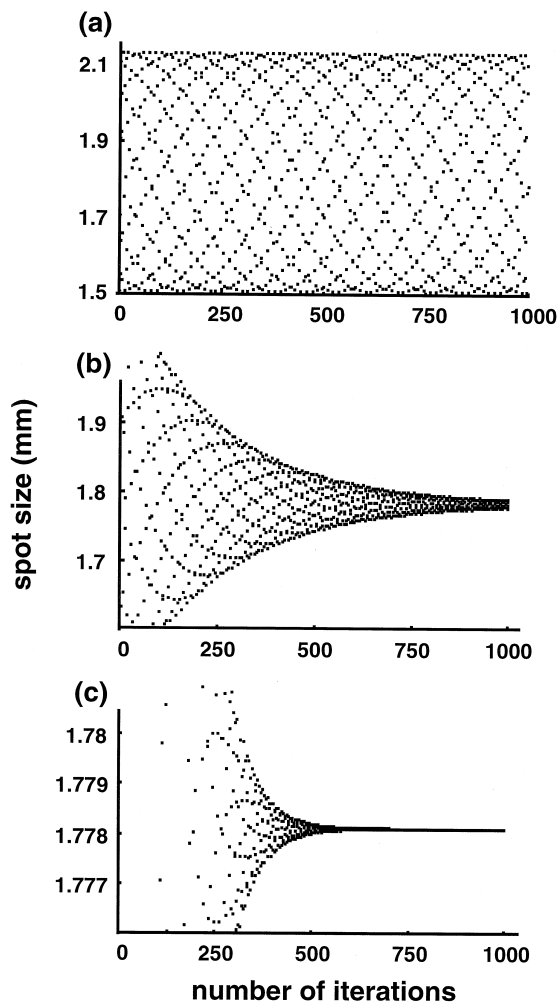


Fig. 5. Evolution of spot size with long period for  $g_1 g_2 = 0.89$ . (a) Conservative system, and with damping of  $a_2 = 10^4 \text{ m}^{-2}$  (b) and  $4 \times 10^4 \text{ m}^{-2}$  (c), respectively.

other two iterations. Fig. 4(a) shows a numerical result of spot size versus number of iterations. The evolution associates with flip-flopping between two values in a smaller scale abscissa for the real transfer matrix system. And the result for a lossy system with  $a_2 = 10^4 \text{ m}^{-2}$  is shown in Fig. 4(b), it acts like a critical damping oscillatory motion and will monotonically converge to its fixed point.

From the concept of classical mechanics, the longer period oscillatory motions have faster overdamping effect than the shorter ones for the same damping parameter. Similar results are found in the evolution of maps. Considering  $g_1 g_2 = 0.89$ , the period of oscillatory trajectory is about 1071 iterations with  $\theta \approx 0.43\pi$  and  $n = 14/3$  in Eq. (9). The period is longer than the one of  $g_1 g_2 = 0.9$ . The spot size evolution without damping is shown in Fig. 5(a). When we add the Gaussian aperture with  $a_2 = 10^4 \text{ m}^{-2}$

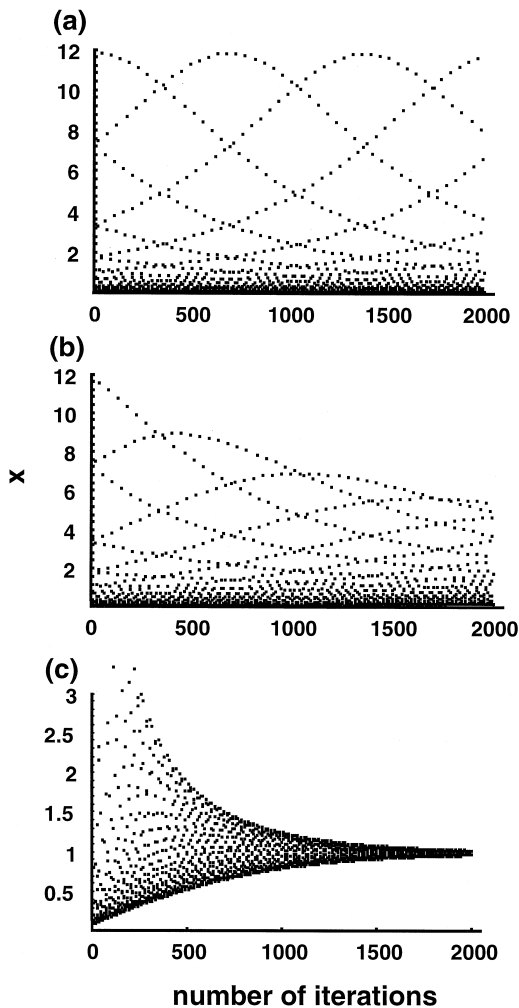


Fig. 6. Evolution of  $x$ , corresponding to spot size, with long period for the Gaussian Schell-model type (GSM) beam in Ref. [2] with  $g = 0.1$ . (a) The Fresnel number,  $F$ , is infinity, (b)  $F = 10000$ , and (c)  $F = 500$ .

which is the same as the value in Fig. 3(c) for  $g_1 g_2 = 0.9$ , the oscillatory motion becomes overdamping as shown in Fig. 5(b). Further increasing the damping parameter to  $a_2 = 4 \times 10^4 \text{ m}^{-2}$ , the evolution shows fast overdamping even before oscillatory motion and has been observed in Fig. 5(c). It is classified as the “quite complicated” evolution in Ref. [2]. But the numerical results display that the “damped oscillation on a few main frequencies” and “quite complicated” evolution in Ref. [2] are just short and long period oscillatory motions, and the “quite complicated” evolution is like the overdamping result having larger damping effect. For verifying this postulation, the numerical results derived from the map of Ref. [2] are shown in Fig. 6. Considering their coherent map with initial values  $(x_0, y_0, c_0) = (0.4, 0.4, 2)$  and  $g = 0.1$ , we plot in Fig. 6(a) the evolution of  $x$  with the Fresnel number,  $F$  equal to infinity. The map corresponds to the conservative one with long period oscillatory motion. When we add a damping effect to the map by setting  $F = 10000$ , the evolution is an underdamping oscillation in Fig. 6(b). Further increase of the damping effect having  $F = 500$ , the evolution shows a “quite complicated” result in Fig. 6(c). The same result can be obtained from initial values of incoherent beam and other  $g$ -value corresponding to the “quite complicated” evolution in Ref. [2]. Therefore, the “damped oscillation on a few main frequencies” and “quite complicated” evolutions have the same dynamic origin and can be explained by the residue and phase shift per iteration of the map in our approach.

For  $g_1 g_2 > 1$ , the iterative spot size becomes divergent without adding Gaussian aperture, it represents that the resonator is unstable and agrees with the previous result from ray tracing [1]. The damping effect causes divergence to be restrained when adding a Gaussian aperture, so the evolution has the same “monotonic” consequence as in Ref. [2].

#### 4. Conclusions

In summary, we had constructed a map from the propagation of beam parameters of a general optical resonator to study its stability and complex dynamics by the residue of the map’s Jacobian matrices. For the lossless resonator having a real round-trip transfer matrix, the residue is a function of the  $g$ -parameters’ product. As a result, besides geometrically stable regions and critical stable borderlines of a linear optical resonator being obtained, we find new dynamically critical stable curves corresponding to  $g$ -parameters’ product equal to  $1/2$ . We think that this configuration is sensitive to the nonlinear effect and contains fruitful nonlinear dynamic properties. Moreover, the dynamic behavior of the dissipative resonator with loss optical element, such as a Gaussian aperture or diffraction loss having complex transfer matrix, is similar to a damping harmonic oscillator. Its intrinsic dynamics complexity

is mainly determined by the system without those loss elements associated with the conservative map.

### Acknowledgements

The research was partially supported by the National Science Council of the Republic of China under grant NSC86-2112-M009-009.

### References

- [1] E. Seigman, Laser, Mill Valley, CA, 1986.
- [2] C. Palma, Optics Comm. 129 (1996) 120.
- [3] A.A. Hnilo, J. Opt. Soc. Am. B 12 (1995) 718.
- [4] J.M. Greene, J. Math. Phys. 20 (1979) 1183.
- [5] M. Nazarathy, J. Shamir, J. Opt. Soc. Am. B 72 (1982) 1398.
- [6] J.A. Arnaud, Beam and Fiber Optics, Academic, New York, 1976, ch. 2.
- [7] A.J. Lichtenberg, M.A. Lieberman, Regular and Chaotic Dynamics, Springer, New York, 1992, Ch. 3.
- [8] W. Demtroder, Laser Spectroscopy, 2nd ed. Springer, Berlin, 1996, ch. 5.
- [9] D.-G. Juang, Y.-C. Chen, S.-H. Hsu, K.-H. Lin, W.-F. Hsieh, J. Opt. Soc. Am. B 14 (7) (1997) to be published.
- [10] N.J. Halas, S.N. Liu, N.B. Abraham, Phys. Rev. A 28 (1983) 2915.
- [11] L.W. Casperson, Appl. Optics 12 (1973) 2434.